Rapid Communications

Morphology and kinetics of random sequential adsorption of superballs: From hexapods to cubes

Pooria Yousefi,[1] Hessam Malmir,[2,*] and Muhammad Sahimi[3,†]

[1]*Faculty of Engineering, Science and Research Branch, Azad University, Tehran 14515-775, Iran*

[2]*Department of Chemical and Environmental Engineering, Yale University, New Haven, Connecticut 06511, USA*

[3]*Mork Family Department of Chemical Engineering and Materials Science, University of Southern California, Los Angeles, California 90089, USA*

(Received 29 May 2019; published 23 August 2019)

Superballs represent a class of particles whose shapes are defined by the domain $|x|^{2p} + |y|^{2p} + |z|^{2p} \leqslant R^{2p}$, with $p \in (0, \infty)$ being the *deformation parameter*. $0 < p < 0.5$ represents a family of hexapodlike (concave octahedral-like) particles, $0.5 \leqslant p < 1$ and $p > 1$ represent, respectively, families of convex octahedral-like and cubelike particles, with $p = 1,\ 0.5$, and ∞ representing spheres, octahedra, and cubes. Colloidal zeolite suspensions, catalysis, and adsorption, as well as biomedical magnetic nanoparticles are but a few of the applications of packing of superballs. We introduce a universal method for simulating random sequential adsorption of superballs, which we refer to as the *low-entropy* algorithm, which is about two orders of magnitude faster than the conventional algorithms that represent *high-entropy* methods. The two algorithms yield, respectively, precise estimates of the jamming fraction $\phi_\infty(p)$ and $\nu(p)$, the exponent that characterizes the kinetics of adsorption at long times t, $\phi_\infty(p) - \phi(p,t) \sim t^{-\nu(p)}$. Precise estimates of $\phi_\infty(p)$ and $\nu(p)$ are obtained and shown to be in agreement with the existing analytical and numerical results for certain types of superballs.

DOI: 10.1103/PhysRevE.100.020602

Random sequential adsorption (RSA) is an irreversible process for generating nonequilibrium packings of nonoverlapping particles, and is considered a very useful model to study and understand the structure of low-temperature phases of matter, as well as particle aggregation and jamming in a wide variety of applications, from granular media [1,2], to heterogeneous materials [3,4] and biological systems [5,6]. The RSA and its kinetics are also among important problems in statistical physics, which have been studied analytically and numerically for various particles and systems [1,5,7–17]. An important property of the RSA is the kinetics of the adsorption that typically approaches a very slow asymptotic saturation limit (jamming) in which no more particles can be added to the packing.

In this Rapid Communication we focus on a special class of particles, the so-called *superballs*, whose possible shapes include a variety of three-dimensional (3D) concave and convex particles. Colloidal zeolite suspensions with applications in catalysis, adsorption, and separation [18,19], as well as packings of magnetic nanoparticles with biomedical applications [20–22] are but some of the better-known applications of the RSA of superballs. Although optimal (lattice) packings and maximally randomly jammed (MRJ) systems of superballs have been studied by Jiao *et al.* [23,24], packing of superballs by the RSA and its kinetics have not been investigated. The importance of modeling and analysis of the RSA of superballs is due to the fact that by tuning a shape parameter (see below) one obtains a wide variety of particle shapes, ranging from hexapod- to octahedral- and cubelike particles, as well as spherical ones. At the same time, determining the saturation coverage and kinetics of the RSA of various types of particles by a unified approach is a long-standing problem, which we address in this Rapid Communication by studying a large family of superballs. One of the main questions that we address is how changing the particles' shape from concave to convex affects the maximum saturation coverage ϕ_∞ (sometimes called the jamming limit) of their packings. From a practical viewpoint, the adsorption rate of the particles is also an important property, which we study and compare with the existing conjectures on the kinetics of the RSA [1,2,5,7,8,10,13,15].

The domain of superballs is described by the following equation:

$$|x - x_{\rm cm}|^{2p} + |y - y_{\rm cm}|^{2p} + |z - z_{\rm cm}|^{2p} \leqslant R^{2p}, \qquad (1)$$

where $p \geqslant 0$ is the *deformation parameter* that indicates the extent to which the particle's shape deviates (deforms) from that of a sphere, the limit $p = 1$, R is the superballs' radius, and subscript cm refers to the center of mass of the particles. Depending on p, a superball may possess two types of shape anisotropy, namely, cubelike and octahedral-like shapes. As p increases from 1 to ∞, one obtains a family of convex superballs with cubelike shapes. The limit $p \to \infty$ represents a perfect cube. As p decreases from 1 to 0.5, a family of convex superballs with octahedral-like shapes are obtained. In the limit $p = 1/2$ the superballs represent regular octahedral particles. For $p < 1/2$, they still possess an octahedral-like shape, but similar to hexapods are concave, and approach a 3D "cross" in the limit $p \to 0$.

*hessam.malmir@yale.edu

†moe@usc.edu

The algorithm that we utilize for simulating the RSA of superballs is a generalization of the one that we recently developed for cubic particles [25–27]. We begin with a large, empty box of volume V in $\mathbf{R}^3$, generate superballs with given deformation parameter p and randomly selected positions and orientations, and place them sequentially in the simulation box. The deposition is subject to the nonoverlapping constraint, so that no newly inserted particles can overlap with any existing ones. The overlap occurrence depends, however, on the spatial coordinates and orientation of the superballs. Thus, the algorithm is as follows. (i) We generate at random the three coordinates $x \in [0, x_{\rm cm}]$, $y \in [0, y_{\rm cm}]$, and $z \in [0, z_{\rm cm}]$ of the superball's center of mass, where $(x_{\max}, y_{\max}, z_{\max})$ are the dimensions of the simulation box. (ii) We generate, for a given value of deformation parameter p, homogeneously distributed surface points according to Eq. (1). To do so, we generate three grid blocks along the three spatial directions and distribute the surface points in only one-eighth of the space, and then use bilateral symmetric mapping to obtain the remaining points in all the directions. (iii) The superball is then rotated using a quaternion [28], $\mathbf{q} = a + b\mathbf{i} + c\mathbf{j} + d\mathbf{k}$, which represents the orientations and rotations of 3D objects. A quaternion is simpler to compose than the Euler's angles that are used to describe the orientation of a rigid body; avoid losing one degree of freedom [29]. (iv) Periodic boundary condition is imposed in all three directions, which checks the surface points on the boundary of the simulation box in order to translate them to proper positions. (v) The surface points of the randomly positioned and rotated superball are checked via Eq. (1) against the centers of the previously inserted superballs to see if any overlap occurs. If so, the superball is rejected and a new one is generated starting from step (i). Otherwise, the superball is accepted and the deposition process continues until the saturation or jamming limit of the system is reached. The number of surface mesh points for all the superballs was about 300, distributed uniformly on the surface of the superballs, and used to check possible overlaps with the center of other existing superballs. In order to do this efficiently, we considered a nearest-neighbor list for each particle and checked the overlap of the generated superballs with its nearest neighbors in its list.

The RSA rate is mainly limited by the volume exclusion from the previously adsorbed particles. Its long-time kinetics is described by [1,10]

$$\phi_\infty(p) - \phi(p,t) \sim t^{-\nu(p)}, \tag{2}$$

in which $\phi(p,t)$ is the packing fraction at dimensionless time t:

$$\phi(p,t) = \frac{n(t)V_{\rm sb}(p)}{V}, \tag{3}$$

and $\phi_\infty(p)$ denotes the RSA maximum saturated packing fraction as $t \to \infty$, with V being the simulation box's volume. $n(t)$ is the number of superballs generated up to time t, and $V_{\rm sb}(p)$ refers to the volume of the superballs [23].

Since the positions of superballs in an RSA packing are equiprobable throughout the simulation box, random sampling of a superball's position follows a uniform probability density function (PDF). Thus, the predictability of the existence of an empty space for inserting a superball, which is a random variable X with a uniform distribution, is controlled by the interval in which the PDF is nonzero, with the simulation box size being $L = \max[x_{\max}, y_{\max}, z_{\max}]$. For $L \to 0$, the PDF becomes a delta function and the predictability is maximal, i.e., the uncertainty is minimum. In this limit, X takes on the value at which the delta function is nonzero. For $L \to \infty$, however, the predictability of the state of X is minimum, i.e., the uncertainty is maximum, and the same is true for all the possible states. Thus, one requires a measure of the uncertainty for the state of the random variable X [30].

Let X be a discrete random variable with possible values $\{x_1, \ldots, x_m\}$ and probabilities $P_i = P(X = x_i)$. The entropy S, a measure of uncertainty, is defined as the expected value of the information gained from observing X [31]:

$$S = -\sum_i P_i \log P_i = \mathcal{E}[-\log P(X)], \tag{4}$$

where $\mathcal{E}$ is the expected value operator. Thus, S depends on the probability distribution of $P_1, \ldots, P_m$, but not on $x_1, \ldots, x_m$. Applying the definition to the RSA in a simulation box of length L yields

$$S = -\int_0^L \frac{1}{L} \ln\left(\frac{1}{L}\right) dx = \ln L, \tag{5}$$

implying that by shrinking the size L of the sampling domain, the uncertainty S of identifying empty space in the RSA also decreases. But, the questions are, how much can one possibly limit the domain of the sampling, and how does it affect the maximum RSA packing fraction ϕ_∞ and its kinetics, which should be independent of the simulation box's dimensions?

To address these questions, we must consider an approach that satisfies the isotropy of the packings and does not alter the RSA constraints. To do so, we propose to first sample the entire simulation box in order to randomly distribute the superballs, and achieve a state in which the number of iterations to find an empty space for inserting a superball becomes very large. We refer to this step as *phase I*. We then divide the simulation box into uniform and equal grid cells, with their size selected such that they can accommodate a few superballs, at least three or four. We then sweep the cells one by one, which we refer to as *phase II*, to more accurately identify any possible empty space that can accommodate new superballs. By decreasing the domain of the sampling in phase II, the predictability of finding empty space for particle insertion increases, ensuring that the true saturation is reached.

We refer to the combination of the two phases as the *low-entropy* RSA, because it is phase II that plays the most important part in the computations. It yields precise estimates for the maximum saturation coverage, $\phi_\infty(p)$. The approach cannot, however, capture accurately and efficiently the kinetics of the RSA because phase II that explores the cells sequentially is a slow process. Thus, it makes reaching the true asymptotic kinetics of the RSA difficult. Hence, we still need to use the conventional RSA, which we refer to as the *high-entropy* RSA process in which phase II is not considered, or has a negligible effect in the simulations and, therefore, almost all the superballs are generated and inserted during phase I. The use of low- and high-entropy terminology is

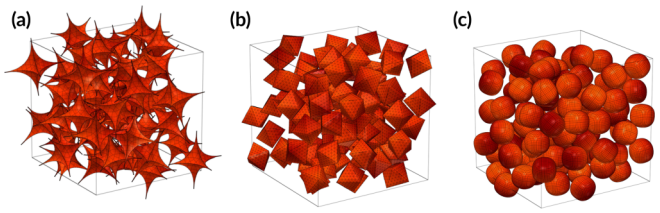

FIG. 1. Packings of (a) concave superballs with $p = 1/4$, (b) octahedral particles with $p = 1/2$, and (c) cubelike particles with $p = 5/4$. The packings are subject to periodic boundary conditions.

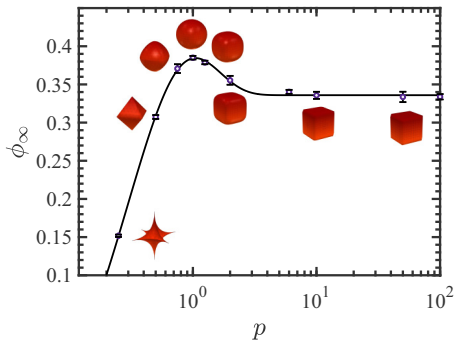

FIG. 2. Maximum RSA packing fractions versus the deformation parameter p. For $p \geqslant 5$, the shape of particles approaches that of cubes with their maximum RSA packing fraction being ∼0.333.

motivated by Eq. (5), according to which by limiting the size L of the domain of sampling the entropy S is kept very low, and there is an absence of this effect in the high-entropy case.

Up to 10^3 superballs were used for each p, and the results were averaged over at least ten realizations. The effect of finite sizes of the simulation box was mitigated by the use of the periodic boundary condition in all directions. To determine the efficiency of the proposed low-entropy algorithm, we carried out a simulation of the RSA of spheres, for which accurate saturation limit is known, determined the average computation time over 100 realizations, and compared the results with those obtained by the conventional RSA simulation. Our simulations, carried out with a 4.0 GHz Intel(R) Core(TM) i7-6700K processor using Visual Studio C^{++}14 compiler, indicated that whereas the average simulation time in the conventional RSA (the high-entropy algorithm) to reach the saturation limit is on the order of a few CPU hours, the low-entropy algorithm takes on average around 40 CPU seconds, so that we have about two orders of magnitude speedup in the computations.

Figure 1 shows three RSA packings. The densest packing is that of cubelike particles with $p = 5/4$ whose shape is still close to spherical particles, the limit $p = 1$. For clear illustration, we show only small portions of each packing in the simulation box. We set $R = 1$ and computed precise estimates of $\phi_\infty(p)$ and the kinetics of adsorption for ten types of superballs, from $p = 1/4$ (concave octahedral-like particles), to $1/2$ (octahedra), $3/4$ (convex octahedral-like particles), and 1 (spheres), as well as six other values of p for the cubelike superballs, using the low-entropy RSA algorithm. The results are shown in Fig. 2. The maximum value of $\phi_\infty(p)$ corresponds to spherical particles for which we obtained $\phi_\infty(p = 1) \approx 0.384\,457 \pm 0.003\,991$, in agreement with the previous estimates, ≈0.382 78 [12], 0.384 130 7 [13], 0.38 [32], and 0.382 [33].

As $p \to 0$, $\phi_\infty(p)$ decreases, with the RSA packing of hexapodlike superballs with $p = 1/4$ having the lowest ϕ_∞ that we computed, $\phi_\infty(p = 1/4) \approx 0.151\,749 \pm 0.001\,553$. Beyond spheres one has cubelike particles with $p > 1$ for which $\phi_\infty(p)$ also decreases, such that for $p > 10$ it reaches the saturation limit, $\phi_\infty(p > 10) \approx 0.333 = 1/3$ for the cubic particles [34]. This is the most accurate estimate of $\phi_\infty(p)$ for the RSA packing of cubes, since preventing overlaps between the particles is based on an overlap potential function, Eq. (1), as $p \to \infty$, and not based on approximations in terms of the edge-edge, edge-face, and corner-face intersections [16]. Note that the same problem also arises for packing of all other polyhedra for which one cannot define an overlap potential function. Here, Eq. (1) is used as an overlap potential function for at least two platonic solids, namely, octahedra ($p = 1/2$) and cubes ($p \to \infty$), not known before.

The plot of $\phi_\infty(p)$ versus p shown in Fig. 2 has a shape distinctly different from that of the lattice and MRJ packings of superballs. Jiao *et al.* [23,24] studied optimal and MRJ packing of superballs, not the RSA. The trends that they reported for $\phi_\infty(p)$ are completely different from what we report here, since for their packings $\phi_\infty(p)$ has its lowest value for the spherical particles, $p = 1$, whereas in the present case the *maximum* of $\phi_\infty(p)$ occurs for $p = 1$. This is a significant result that demonstrates the fundamentally different nature of the structure of the two types of packings, and the fact that the RSA is a process completely different from those that generate dense equilibrated configurations of superballs. The list of estimates of $\phi_\infty(p)$ along with their standard errors, computed by using the low-entropy RSA, is presented in Table I. The fitted curve in Fig. 2 may be approximated by

$$\phi_\infty(p) = C_1 \exp(-C_2 p) \cos(C_3 p - C_4) + C_5, \qquad (6)$$

with $C_1 - C_5$ being, respectively, ≈1.661, 2.089, 0.567, 1.901, and 0.336, which can be used for quickly estimating $\phi_\infty(p)$ for any value of p that we have not studied in this Rapid Communication.

To obtain accurate results for the kinetics of the RSA packing, Eq. (2), we use the high-entropy RSA algorithm.

TABLE I. Maximum packing fraction $\phi_\infty(p)$ of superballs versus the deformation parameters p [35].

p	$\phi_\infty(p)$
1/4	0.151749 ± 0.001553
1/2	0.307333 ± 0.002553
3/4	0.370720 ± 0.005747
1	0.384457 ± 0.003991
5/4	0.378758 ± 0.002304
2	0.355377 ± 0.005804
6	0.340227 ± 0.002650
10	0.335687 ± 0.004656
50	0.333634 ± 0.006789
100	0.333832 ± 0.003552

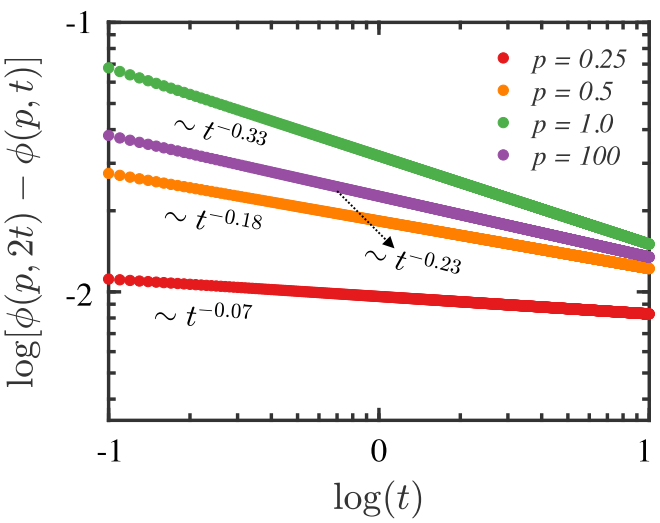

FIG. 3. The kinetics of the RSA for various deformation parameters p. The asymptotic behavior of $\log[\phi(p,2t)-\phi(p,t)]$ that exhibits the same scaling as $\log[\phi_\infty(p)-\phi(p,t)]$ when plotted against $\log(t)$ [Eq. (2)]. Purple, green, and orange indicate, respectively, cubes, spheres, and octahedra, while red represents hexapodlike particles with $p = 1/4$.

Figure 3 shows the dependence of $\phi(p,2t)-\phi(p,t)$ on the dimensionless time t defined by $t = n_i V_{\rm sb}(p)/V$ in which n_i denotes the number of RSA iterations, i.e., the number of successive additions of the particles. Since it is not practical to carry out the simulations for too long, we derive the asymptotic behavior by analyzing $\log[\phi(p,2t)-\phi(p,t)]$ that exhibits the same scaling as $\log[\phi_\infty(p)-\phi(p,t)]$, when plotted against $\log(t)$ [15]. As illustrated, the slope of $\log[\phi(p,2t)-\phi(p,t)]$, which corresponds to $-\nu(p)$ in Eq. (2), has its maximum and minimum values at, respectively, $p = 1$ (spheres) and $p = 1/4$ (hexapodlike superballs). For spherical particles, one has $\nu(p=1) \approx 0.33$, which was previously predicted [5,7,8,12,30]. For cubes and octahedra, however, $\nu(p) \approx 0.23$ and 0.18, respectively. The plot of $\log[\phi_\infty(p)-\phi(p,t)]$ with respect to $\log(t)$ decays slowly for concave octahedral-like particles. For $p = 1/4$ we obtain $\nu \approx 0.07$. In this limit, the relation $\phi_\infty(1/4)-\phi(1/4,t) \sim \log(t)$ also quantifies the asymptotic behavior extremely accurately, which is not surprising as ν is very small.

To further characterize the structure of the RSA packings, we computed the pair correlation function $g_2(r)$ at $\phi_\infty(p)$. Figure 4 presents the results. The peak of $g_2(r)$ occurs at $r = D$ for the spherical particles, where $D = 2R$ is the superballs' diameter, and moves from left to right with increasing p. Since for superballs with $p < 1$ the diameter D equals the diameter of their circumscribed sphere, Fig. 4 indicates that for $p = 1/4$ and $p = 1/2$ (octahedron) and $r < D$ we still have some neighboring superballs around the reference one,

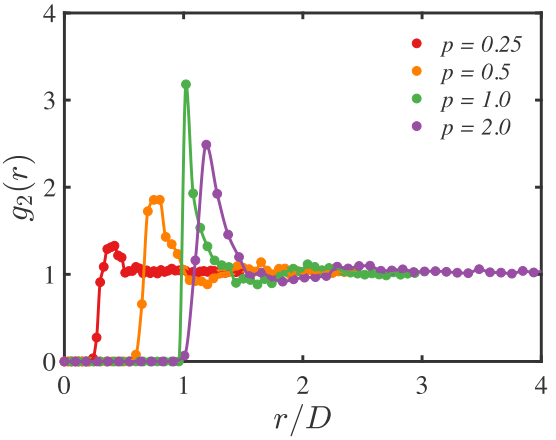

FIG. 4. The pair-correlation function $g_2(r)$ for the RSA packing of superballs at ϕ_∞. Purple, green, and orange show, respectively, cubelike particles ($p = 2$), spheres ($p = 1$), and octahedra ($p = 1/2$), while red represents the results for hexapodlike particles ($p = 1/4$). The peak of $g_2(r)$ moves from left to right as the deformation parameter p increases. For spherical particles, $\lim_{r\to D^+} g_2(r) \sim -\ln(r/D-1)$.

but the peak of $g_2(r)$ occurs at smaller r for smaller p, and has lower values for such values of p. In fact, for $p < 1$ the center of the superballs may be closer than the diameter of their circumscribed sphere.

On the other hand, for superballs with $p > 1$ the diameter D is the diameter of their inscribed sphere, which is why the peak of $g_2(r)$ in Fig. 4 for $p = 2.0$ (cubelike particles) occurs at $r > D$, although the peak's value is still lower than that of spheres ($p = 1$). This is due to the fact that for $p > 1$ the center-to-center distance of the superballs is greater than the diameter of their inscribed sphere. Furthermore, the limiting values for $g_2(r)$ of spheres are similar to those of Refs. [7,8,12,13], namely, $\lim_{r\to D^+} g_2(r) \sim -\ln(r/D-1)$, which supports the conjecture on the logarithmic singularity of $g_2(r)$ at $r = D$ for spherical particles.

Summarizing, by developing a simulation algorithm, we carried out a comprehensive study of the RSA of superballs. The maximum packing fraction and the kinetics of the adsorption were studied and the relevant quantities were estimated. We proposed an efficient universal computational approach, namely, the low-entropy process that leads to the precise estimates of the jamming. The highest saturated packing fraction among superballs belongs to spherical particles ($p = 1$). Both the long-time kinetics and the pair-correlation function $g_2(r)$ of the RSA of superballs at $p = 1$ support the previous conjectures on the RSA of spherical particles.

Work at USC was supported in part by the Petroleum Research Fund, administered by the American Chemical Society. H.M. gratefully acknowledges useful discussions with Adrian Baule.

[1] J. W. Evans, Random and cooperative sequential adsorption, Rev. Mod. Phys. **65**, 1281 (1993).

[2] S. Torquato and F. H. Stillinger, Jammed hard-particle packings: From Kepler to Bernal and beyond, Rev. Mod. Phys. **82**, 2633 (2010).

[3] S. Torquato, *Random Heterogeneous Materials* (Springer, New York, 2002).

[4] M. Sahimi, *Heterogeneous Materials I* (Springer, New York, 2003).

[5] J. Feder, Random sequential adsorption, J. Theor. Biol. **87**, 237 (1980).

[6] J. Talbot, G. Tarjus, P. V. Tassel, and P. Viot, From car parking to protein adsorption: An overview of sequential adsorption processes, Colloids Surf., A **165**, 287 (2000).

[7] Y. Pomeau, Some asymptotic estimates in the random parking problem, J. Phys. A **13**, L193 (1980).

[8] R. H. Swendsen, Dynamics of random sequential adsorption, Phys. Rev. A **24**, 504 (1981).

[9] E. L. Hinrichsen, J. Feder, and T. Jøssang, Random packing of disks in two dimensions, Phys. Rev. A **41**, 4199 (1990).

[10] P. Viot and G. Tarjus, Random sequential addition of unoriented squares: Breakdown of Swendsen's conjecture, Europhys. Lett. **13**, 295 (1990).

[11] J.-S. Wang and R. B. Pandey, Kinetics and Jamming Coverage in a Random Sequential Adsorption of Polymer Chains, Phys. Rev. Lett. **77**, 1773 (1996).

[12] S. Torquato, O. U. Uche, and F. H. Stillinger, Random sequential addition of hard spheres in high Euclidean dimensions, Phys. Rev. E **74**, 061308 (2006).

[13] G. Zhang and S. Torquato, Precise algorithm to generate random sequential addition of hard hyperspheres at saturation, Phys. Rev. E **88**, 053312 (2013).

[14] Y. Y. Tarasevich, V. V. Laptev, N. V. Vygornitskii, and N. I. Lebovka, Impact of defects on percolation in random sequential adsorption of linear k-mers on square lattices, Phys. Rev. E **91**, 012109 (2015).

[15] A. Baule, Shape Universality Classes in the Random Sequential Adsorption of Nonspherical Particles, Phys. Rev. Lett. **119**, 028003 (2017).

[16] M. Ciésla and P. Kubala, Random sequential adsorption of cubes, J. Chem. Phys. **148**, 024501 (2018).

[17] G. Zhang, Precise algorithm to generate random sequential adsorption of hard polygons at saturation, Phys. Rev. E **97**, 043311 (2018).

[18] P. Sharma, J.-S. Song, M. H. Han, and C.-H. Cho, GIS-NaP1 zeolite microspheres as potential water adsorption material: Influence of initial silica concentration on adsorptive and physical/topological properties, Sci. Rep. **6**, 22734 (2016).

[19] S. Li, J. Li, M. Dong, S. Fan, T. Zhao, J. Wang, and W. Fan, Strategies to control zeolite particle morphology, Chem. Soc. Rev. **48**, 885 (2019).

[20] G. Salazar-Alvarez, J. Qin, V. Sepelák, I. Bergmann, M. Vasilakaki, K. N. Trohidou, J. D. Ardisson, W. A. A. Macedo, M. Mikhaylova, M. Muhammed, M. D. Baró, and J. Nogués, Cubic versus spherical magnetic nanoparticles: The role of surface anisotropy, J. Am. Chem. Soc. **130**, 13234 (2008).

[21] J. Zhang, J. Du, Y. Qian, Q. Yin, and D. Zhang, Shape-controlled synthesis and their magnetic properties of hexapod-like, flake-like and chain-like carbon-encapsulated Fe_3O_4 core/shell composites, Mater. Sci. Eng., B **170**, 51 (2010).

[22] J. G. Donaldson, P. Linse, and S. S. Kantorovich, How cube-like must magnetic nanoparticles be to modify their self-assembly? Nanoscale **9**, 6448 (2017).

[23] Y. Jiao, F. H. Stillinger, and S. Torquato, Optimal packings of superballs, Phys. Rev. E **79**, 041309 (2009).

[24] Y. Jiao, F. H. Stillinger, and S. Torquato, Distinctive features arising in maximally random jammed packings of superballs, Phys. Rev. E **81**, 041304 (2010).

[25] H. Malmir, M. Sahimi, and M. R. Rahimi Tabar, Microstructural characterization of random packings of cubic particles, Sci. Rep. **6**, 35024 (2016).

[26] H. Malmir, M. Sahimi, and M. R. Rahimi Tabar, Packing of nonoverlapping cubic particles: Computational algorithms and microstructural characteristics, Phys. Rev. E **94**, 062901 (2016).

[27] H. Malmir, M. Sahimi, and M. R. Rahimi Tabar, Statistical characterization of microstructure of packings of polydisperse hard cubes, Phys. Rev. E **95**, 052902 (2017).

[28] J. Conway and D. Smith, *On Quaternions and Octonions* (Taylor & Francis, London, 2003).

[29] E. G. Hemingway and O. M. O'Reilly, Perspectives on Euler angle singularities, gimbal lock, and the orthogonality of applied forces and applied moments, Multibody Syst. Dyn. **44**, 31 (2018).

[30] S. Heinz, *Mathematical Modeling* (Springer, Berlin, 2011).

[31] M. Kelbert and Y. Suhov, *Information Theory and Coding by Example* (Cambridge University Press, London, 2013).

[32] D. W. Cooper, Random-sequential-packing simulations in three dimensions for spheres, Phys. Rev. A **38**, 522 (1988).

[33] J. Talbot, P. Schaaf, and G. Tarjus, Random sequential addition of hard spheres, Mol. Phys. **72**, 1397 (1991).

[34] In Refs. [25,26] the estimate $\phi_\infty \approx 0.57$ was reported for the RSA packings of cubes. The estimate was, however, erroneous because upon repeating the calculations with the present method it was discovered that even very small overlaps between the particles, as small as 1%–2%, change ϕ_∞ very significantly. The estimate we present here agrees with that of Ref. [16].

[35] See https://en.wikipedia.org/wiki/Random_sequential_adsorption for a list of estimates of ϕ_∞ for a variety of particles in both 2D and 3D.